Molecular Therapy
Oncology
Original Article

Exclusion of PD-1 from the immune synapse: A novel strategy to modulate T cell function

Luke Yi Hao,[1,5] Shalom Lerrer,[1,5] Matthieu Paiola,[1] Emily K. Moore,[1] Yevgeniya Gartshteyn,[1,2] Ruijiang Song,[1] Michael Goeckeritz,[1,3] Matilda J. Black,[1,4] Shoiab Bukhari,[1] Xizi Hu,[1] and Adam Mor[1,2]

[1]Columbia Center for Translational Immunology, Columbia University Medical Center, New York, NY 10032, USA; [2]Division of Rheumatology, Department of Medicine, Columbia University Medical Center, New York, NY 10032, USA; [3]Institute of Anatomy and Cell Biology, Faculty of Medicine, Martin Luther University Halle-Wittenberg, 06108 Halle, Germany; [4]Department of Medicine, Faculty of Biology, University of Cambridge, CB2 1TN Cambridge, UK

Targeting immune checkpoint receptors on T cells is a common cancer treatment strategy. Frequently, this is accomplished through antibodies targeting the ligand of inhibitory co-receptors. Blocking the immune checkpoint PD-1 binding to its ligands PD-L1 and PD-L2 prevents downstream signaling and enhances anti-tumor T cell responses. This approach improves cancer patients' outcomes. However, only one-third of the patients respond to these treatments. To better understand the mechanism of anti-PD-1 antibodies, we explored the location of PD-1 within the immune synapse. Surprisingly, we discovered that anti-PD-1 antibodies, besides blocking the interaction between PD-1 and its ligands, also removed PD-1 from the synapse. We demonstrated a correlation between removing PD-1 from the synapse by anti-PD-1 antibodies and the extent of T cell activation. Interestingly, a short version of the anti-PD-1 antibody, $F(ab')_2$, failed to remove PD-1 from the synapse and activate T cells. Using the syngeneic tumor model, we showed a superior anti-tumor effect of the anti-PD-1 antibody over the shorter version of the same antibody. Our data indicate that anti-PD-1 antibodies activate T cells by removing PD-1 from the synapse, and changing the location of PD-1 or other immune receptors within the immune synapse could serve as an alternative, efficient approach to treat cancer.

INTRODUCTION

Antigen-mediated T cell receptor (TCR) activation depends on the prolonged, stable interaction between a T cell and an antigen-presenting or target cell. The interface between these interacting cells is termed the immune synapse (IS), and it includes well-organized supramolecular activation clusters (SMACs).[1] SMACs are concentric rings of segregated proteins sorted by structure and function and driven by the TCR and co-receptor signaling. This structure is essential for proper protein-protein interactions, and the relative proximity between individual proteins within these regions is critical to cellular function. For example, the central SMAC is enriched in co-receptors, such as CD4, CD8, CD28, and PD-1; the peripheral SMAC (p-SMAC) is increased in LFA-1/ICAM-1 interaction; and the distal SMAC (d-SMAC) is enriched in F-actin and the transmembrane phosphatases CD45 and CD43.[2]

There is a tight space between these interacting cells, created by integrin-adhesion molecule interactions, and the size-based exclusion of molecules from the IS has been reported previously.[3,4] According to a crystal structure analysis of the IS, the intermembrane distance for receptor-ligand pairs is approximately 15 nm and about 40 nm for integrin-ligand pairs.[5,6] Using a range of sizes of dextran molecules, it was established that the movement of dextran molecules $\leq$ 4 nm in and out of the IS was unrestricted. However, the direction of 10- to 13-nm dextran molecules was significantly reduced, and dextran molecules above 32 nm were nearly completely excluded.[7] Further, monoclonal antibodies that correspond to a size of around 15 nm were also excluded from the IS.[8]

Targeting immune checkpoints on the surface of T cells is a prevailing approach in cancer immunotherapy.[9] Most immune checkpoint inhibitors, monoclonal antibodies, operate through an assumed mechanism of disrupting receptor-ligand interactions. Antibodies directed toward PD-1, the PD-1 ligand PD-L1, lymphocyte-activation gene 3 (LAG-3), T cell immunoglobulin and mucin domain-containing protein 3 (TIM3), T cell immunoreceptor with Ig and ITIM domains (TIGIT), and CTLA-4 fall under this category.[10] While these antibodies achieve blockade of receptor-ligand interactions and interfere with outside-in signaling, emerging data suggest that this may not be the sole explanation for their efficacy.[11] Further exploring alternative mechanisms to achieve immune checkpoint inhibition promises to expand patient responsiveness and address primary resistance and immune-related adverse events.[12]

Because full-length antibodies cannot enter the tight space of the IS, we hypothesized that anti-PD-1 antibodies bind to PD-1 and pull it away from the IS, disrupting the signaling complexes within the synapse. To test this hypothesis, we imaged T cells that express GFP-tagged PD-1 before and after treatment with anti-PD-1

Received 31 October 2023; accepted 14 June 2024;
https://doi.org/10.1016/j.omton.2024.200839.

[5]These authors contributed equally

Correspondence: Adam Mor, Columbia Center for Translational Immunology, Columbia University Medical Center, New York, NY 10032, USA.
E-mail: am5121@cumc.columbia.edu

Published by Elsevier Inc. on behalf of The American Society of Gene and Cell Therapy.
This is an open access article under the CC BY-NC-ND license (http://creativecommons.org/licenses/by-nc-nd/4.0/).

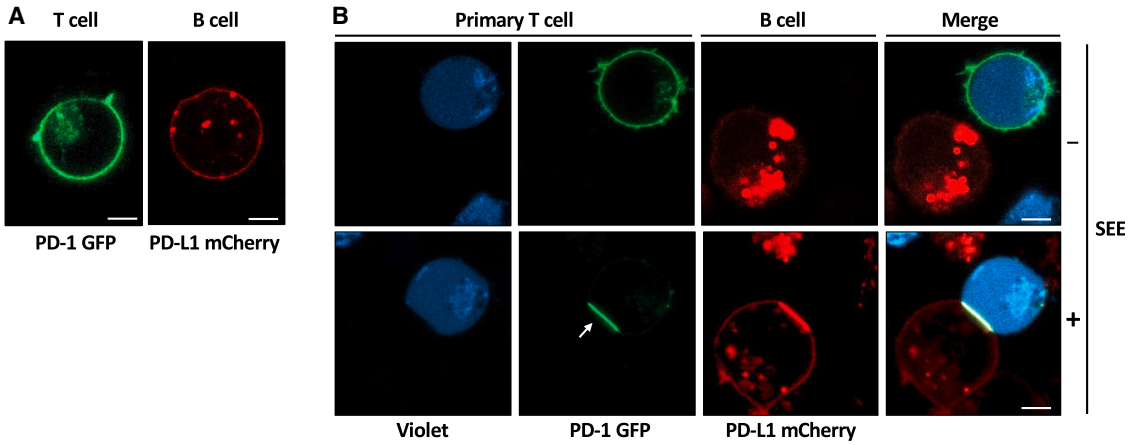

Figure 1. PD-1 is localized to the IS

Primary human T cells expressing GFP-PD-1 co-cultured at rest (A) and with SEE-loaded Raji B cells that expressed mCherry PD-L1 (B). Cells were imaged alive; representative cells are shown.

antibodies and recorded PD-1 location and function through *in vitro* and *in vivo* systems.

RESULTS

PD-1 is localized to the IS

To gain better insight into the location of PD-1 in the IS, we overexpressed GFP-PD-1 in primary human T cells and co-cultured these cells with staphylococcal enterotoxin E (SEE)-loaded Raji B cells that expressed mCherry PD-L1, as reported previously.[13] PD-1 was homogenously distributed around the cells during the resting state (Figure 1A) but localized to the IS in the activated cells (Figure 1B).

Full-length anti-PD-1 antibodies removed PD-1 from the IS

It has been reported that antibodies cannot enter the tight IS due to their size.[14] Indeed, we have reported that anti-PAG[13,15] and anti-SLAMF6[16,17] antibodies, due to their size, cannot populate the IS. Thus, we hypothesized that PD-1 is removed from the IS during conjugate formation in the setting of anti-PD-1 antibodies. First, we treated nivolumab (anti-PD-1 antibody) with pepsin to generate $F(ab')_2$ (Figure 2A). Next, we used flow cytometry to show that nivolumab $F(ab')_2$ can bind to T cells expressing PD-1 with the same affinity as a full-length nivolumab (Figure 2B). To better control the experiment, we also treated durvalumab, an anti-PD-L1 antibody, with pepsin to generate $F(ab')_2$ (Figure 3A) and showed that its affinity to PD-L1 was maintained (Figure 3B). Next, we treated GFP-PD-1 expressing Jurkat T cells and SEE-loaded Raji B cells expressing mCherry PD-L1 with nivolumab and its $F(ab')_2$ (Figure 2Ci) or with durvalumab and its $F(ab')_2$ (Figure 3Ci). We quantified the number of cells where PD-1 was recruited to the IS (Figure S1) at different concentrations of both antibodies. As shown, while nivolumab could remove PD-1 from the synapse in most of the cells, its $F(ab')_2$ failed to do that (Figure 2Cii). Similar results were quantified using durvalumab (Figure 3Cii). An analogous pattern was observed on primary human T cells for nivolumab and its $F(ab')_2$ (Figure 2D). As a control, an isotype control antibody failed to remove PD-1 from the synapse in 95% of the cells (Figure 2E). To better visualize the synapse, we obtained a z stack image to model the IS in three dimensions. In the experiment with the full-length nivolumab, PD-1 molecules were located at the rim of the synapse (Figure 2F, left). In contrast, in the nivolumab $F(ab')_2$ treatment experiment, PD-1 molecules were still localized at the center of the synapse (Figure 2F, right). Altogether, these data suggested that an anti-PD-1 antibody, besides blocking its binding to PD-L1, can also remove its target from the IS.

Removing PD-1 from the IS is associated with increased T cell activation

To uncover the biological significance of removing PD-1 from the synapse, we treated Jurkat T cell and Raji B cell with different concentrations of either full-length nivolumab or its $F(ab')_2$ in the context of SEE (Figure 4A). The culture medium was collected after overnight treatment, and ELISA measured interleukin-2 (IL-2) levels. As shown, unlike full-length nivolumab, nivolumab $F(ab')_2$ could not effectively increase the levels of secreted IL-2. Next, we repeated the same procedure with human peripheral blood mononuclear cells (PBMCs). Only full-length nivolumab treatment resulted in increased levels of IL-2 (Figure 4B, left) and interferon-gamma (Figure 4B, right), two cytokines secreted from activated T cells in response to tumors. To uncover the molecular mechanism and to link our findings of PD-1 signaling, we treated the cells with either full-length nivolumab or nivolumab $F(ab')_2$ for 5 min, cocultured the cells, and then precipitated PD-1 with anti-GFP antibodies and blotted the precipitate with anti-4G10 antibodies to quantify the levels of the PD-1 endo domain tyrosine phosphorylation. While nivolumab $F(ab')_2$ reduced the levels of PD-1 phosphorylation to baseline, the full-length nivolumab reduced PD-1 phosphorylation levels even further (Figures 4Ci and 4Cii), suggesting that tonic signaling downstream of PD-1 can be inhibited not exclusively by interfering with ligand binding but by physically removing it from the synapse.

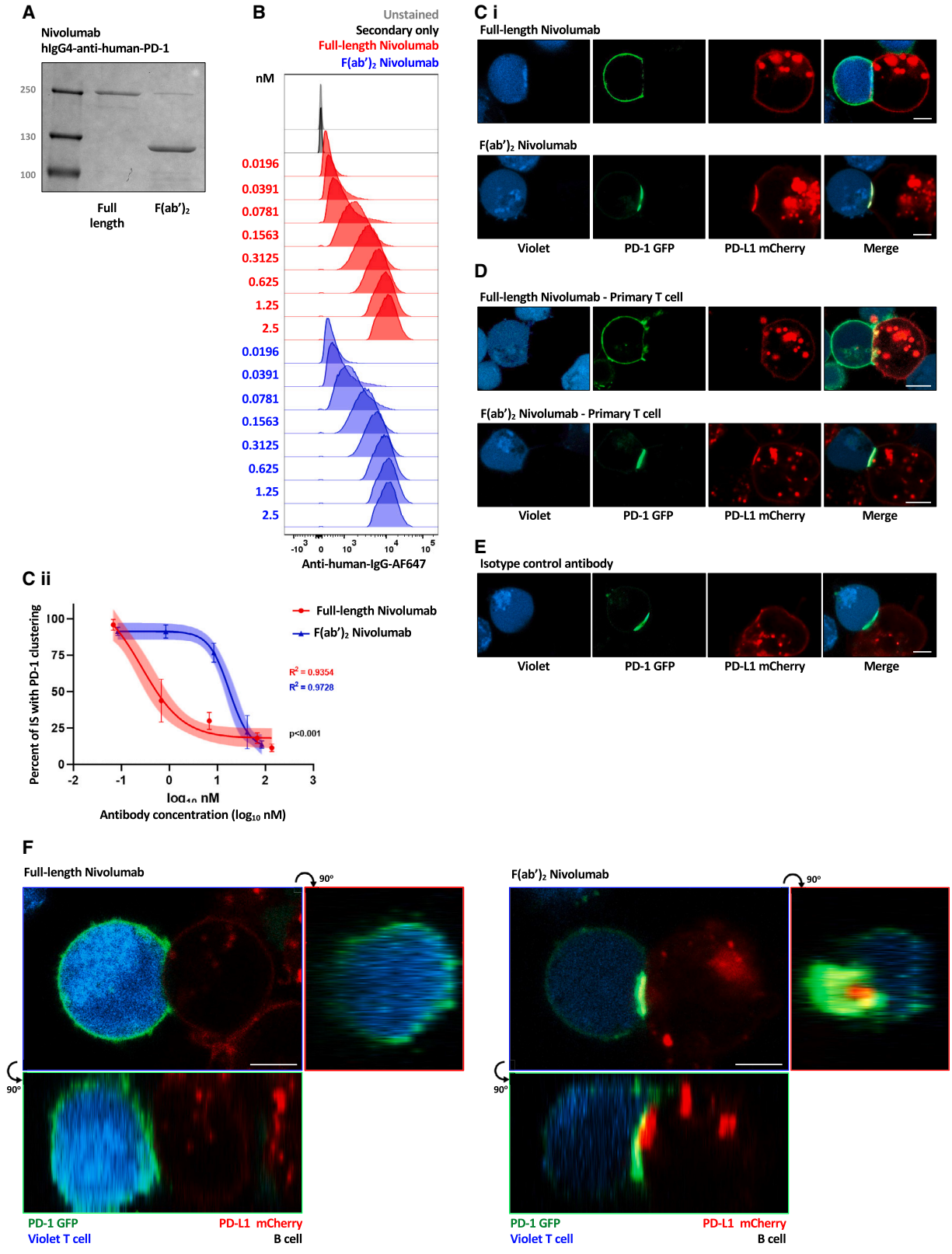

(legend on next page)

Anti-PD-1 F(ab′)$_2$ cannot inhibit tumor growth *in vivo*

To test the role of the anti-PD-1 antibody and its F(ab′)$_2$ *in vivo*, we treated the anti-murine PD-1 antibody with pepsin (Figure 5A) and confirmed its affinity using an EL4 murine T cell line (Figure 5B). Next, we used the MC38 syngeneic colon adenocarcinoma tumor model to test the ability of the antibodies to reduce tumor growth. MC38-inoculated mice were treated with full-length anti-PD-1 antibodies twice a week for four doses or with the same molar amount of anti-murine PD-1 F(ab′)$_2$. As shown, the tumors grew faster when the short version of anti-PD-1 was used (Figure 5C). H&E staining of the tumors at the end of the experiment confirmed an increased number of tumors infiltrating T cells in the mice treated with full-length antibodies (Figure 5D). Remarkably, both the full-length and the F(ab′)$_2$ versions of the anti-PD-1 antibodies were detected at the same level on T cells isolated from the spleens of these mice 2 weeks after the intraperitoneal administration (Figure 5E).

DISCUSSION

The PD-1 pathway provides a clear example of how changing a protein's localization on the cell surface can impact T cell function. During T cell activation, the TCR localizes within micro-clusters within the IS and the PD-1.[18] It is well established that PD-1 interacts with Src homology 2 (SH2) domain-containing proteins upon ligation through phosphorylated tyrosines within its intracellular tail. More specifically, two tyrosine motifs, an immunoreceptor tyrosine-based inhibitory motif and an immunoreceptor tyrosine-based switch motif, are contained within the cytoplasmic tail of PD-1 and become phosphorylated following PD-1 ligation.[19] If PD-1 were re-localized away from the TCR, then the proximity of its cell-surface and intracellular binding partners and the TCR would also be disrupted. As a result, these proximity-dependent inhibitors will be unable to act on the TCR cascade, and T cell activation will be enhanced. Perhaps the most well-studied PD-1-interacting protein is the SH2 domain-containing tyrosine phosphatase 2 (SHP2), which binds to the phosphorylated cytoplasmic tail of PD-1. We have demonstrated previously that the immunoreceptor tyrosine-based switch motif (ITSM) and immunoreceptor tyrosine-based inhibitory motif (ITIM) contribute to SHP2 localization and full activation.[20,21] Once activated, SHP2 dephosphorylates critical tyrosine signaling mediators within the CD3 complex and CD28, ZAP70, phosphatidylinositol 3-kinase, protein kinase B (AKT), C3G, and extracellular signal-regulated kinases (ERK).[22,23] By removing PD-1 from the TCR microclusters, SHP2 will be mislocalized and remain inactive.

We have shown here that anti-PD-1 monoclonal antibodies block PD-1 interaction with PD-L1 by changing the location of PD-1 away from the p-SMAC toward the d-SMAC. Mechanistically, this is explained by the tight and narrow space between the T cell and the tumor cells, which cannot accommodate the bulky Fc portion of most therapeutic antibodies. Previously, another group showed anti-PD-1 F(ab′′)$_2$-conjugated pegylated (PEG)-poly(lactic-co-glycolic acid) (PLGA) nanoparticles enhance immune checkpoint therapy in the same MC38 syngeneic mouse tumor model.[24] We suspected that their average bulky size of 260 nm significantly affected the anti-tumor efficacy. To further support that, we were able to show a correlation between the degree of PD-1 exclusion from the IS and its lack of ability to prevent cell proliferation and cytokine secretion. It has been suggested that resistance to PD-1 blockade, at least partially, is secondary to incomplete hindering of PD-1. We recommend addressing incomplete responses to current anti-PD-1 antibodies by using modified anti-PD-1 antibodies that can remove PD-1 away from the IS. Another advantage of this approach is its ability to prevent PD-1 ligand-independent downstream tonic signaling.[25] Since the ability to remove PD-1 from the synapse is not the same as that of all antibody isotypes, this property should be considered for developing next-generation anti-PD-1 therapeutics.

Immunotherapies have changed the way we treat patients with cancer. Most of the targets of these therapies are co-receptors expressed on the surface of T cells that are members of the IS.[26] The synapse is a dynamic platform that can initiate downstream signaling by two mechanisms. The first is enabling receptors on T cells to bind to ligands on the target cells, promoting outside-in signaling, or "vertical signaling."[27] The other mechanism is the formation of signaling clusters between proteins located within the membrane of the T cells, a process conceptualized as "horizontal signaling."[28,29] The formation of such groups can lead to ligand-independent downstream signaling that could either stimulate or inhibit T cell functions. For example, antibodies to PD-1 block ligand binding and outside-in signaling. However, we have demonstrated that PD-1 inhibition by antibodies may go beyond ligand neutralization. Additional inhibition of this pathway could be accomplished by physically removing PD-1 from the synapse, which also interferes with its horizontal signaling (Figure 5F). We have demonstrated that moving the adaptor protein PAG away from the IS enhances T cell activation and diminishes PD-1 signaling.

Here, we propose a new design of antibodies targeting proteins in the IS with bulkier sizes, hoping to increase their effectiveness.[30] Our tumor model experiment supports this concept. However, future work is needed to determine the upper limit of the antibody's hydrodynamic size. This study proved that an antibody's physical property can

Figure 2. Full-length anti-PD-1 antibodies removed PD-1 from the IS

(A) Coomassie staining of non-reduced full-length nivolumab and nivolumab treated with pepsin. (B) A flow cytometry graph of Jurkat T cells treated with full-length nivolumab and nivolumab F(ab′)$_2$ at different doses, showing the binding affinity of the different versions of the antibodies to the cells. This experiment was done three times, and representative data are shown. (Ci and Cii) GFP-PD-1-expressing Jurkat T cells co-cultured with SEE-loaded Raji B cells expressing mCherry PD-L1 treated with nivolumab and its F(ab′)$_2$ (Ci) and quantification of the number of cells where PD-1 was recruited to the IS at different concentrations of both antibodies (Cii). $n = 5$, $p < 0.001$ (unpaired t test with Welch's correction between the non-linear fitting curves). (D) GFP-PD-1-expressing primary human T cells co-cultured with SEE-loaded Raji B cells expressing mCherry PD-L1 treated with nivolumab and its F(ab′)$_2$. (E) GFP-PD-1 expressing Jurkat T cells co-cultured with SEE-loaded Raji B cells expressing mCherry PD-L1 treated with an isotype control antibody. (F) Z stack-based three-dimensional reconstruction images of Jurkat T cells expressing GFP-PD-1 co-cultured with SEE-loaded Raji B cells expressing mCherry PD-L1 and treated as indicated.

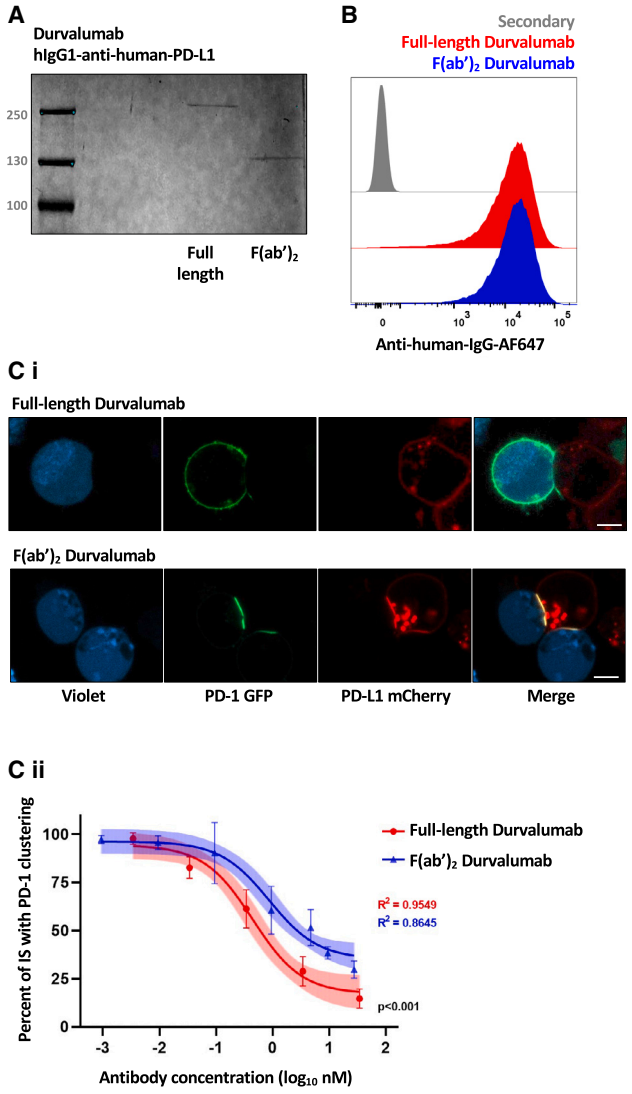

Figure 3. Full-length anti-PD-L1 antibodies removed PD-1 from the IS

(A) Coomassie staining of non-reduced full-length durvalumab and durvalumab treated with pepsin. (B) Flow cytometry of Raji B cells treated with full-length durvalumab and durvalumab F(ab′)$_2$, as indicated. (Ci) GFP-PD-1-expressing Jurkat T cells co-cultured with SEE-loaded Raji B cells expressing mCherry PD-L1 treated with durvalumab and its F(ab′)$_2$ and quantification of the number of cells where PD-1 was recruited to the IS at different concentrations of both antibodies (Cii). $n = 3$, $p < 0.001$ (unpaired t test with Welch's correction between the non-linear fitting curves).

impact its effectiveness. In the future, other physical properties, such as binding affinity, hinge flexibility, and electrostatic charge, can also be explored.

MATERIALS AND METHODS

General reagents

RPMI 1640, DMEM, Dulbecco's PBS, penicillin/streptomycin, and fetal bovine serum (FBS) were purchased from Life Technologies. Lymphoprep was purchased from STEMCELL Technologies. SEE was purchased from Toxin Technology (ET404).

Cell culture and stimulation

Jurkat T cells and Raji B cells were obtained from the American Type Culture Collection (TIB-152 and CCL-86). These cells were maintained in 5% CO_2 at 37°C in RPMI 1640 supplemented with 10% FBS and 1% penicillin/streptomycin. Jurkat T cells and Raji cells were stably expressing the pHR-PD-1-GFP vector and pHR-PD-L1-mCherry vector, respectively, as described previously.[31] The imaging experiments combined Jurkat T and Raji B cells with a 1:1 ratio. For immunoprecipitation for phosphorylated PD-1 levels, Jurkat T cells and Raji B cells were mixed with a 3:1 ratio. Peripheral blood was collected from healthy adult donors following informed consent. Total $CD3^+$ T cells were isolated by density gradient centrifugation (Lymphoprep) and negative selection using the RosetteSep human T cell enrichment mixture (STEMCELL Technologies). *In vitro*, T cell cultures were maintained in complete RPMI medium containing 10% fetal calf serum, minimum Eagle's medium nonessential amino acids, 1 mM sodium pyruvate, 100 IU/mL penicillin, 100 μg/mL streptomycin, and GlutaMAX-I. Amaxa nucleofection was used to transiently express GFP-PD-1 in $CD3^+$ primary human T cells (Lonza).

Imaging and microscopy

Raji B cells (1 million cells/mL) loaded with 0.1 μg/mL SEE were co-cultured with Jurkat T cells (1 million cells/mL) with a 1:1 ratio before being treated with the nivolumab and durvalumab antibodies. For conjugate experiments, live-cell co-cultures were imaged for 30 min using confocal microscopy (Carl Zeiss, LSM 900). IS and PD-1 clustering were counted in ZEN 3.3 (blue edition) for quantification (Figure S1). In each experiment, blinded microscopists counted more than 100 conjugates. Each experiment was repeated at least three times.

Antibody processing and validation

Clinical-grade nivolumab fragments, clinical-grade durvalumab fragments, and rat-anti-mouse-PD-1 antibody (catalog number BE0146, InVivoMAb) were prepared by Pierce F(ab′)2 Macro Preparation Kit (catalog number 44988). The sizes of antibody fragments were measured through non-reducing Tris-glycine PAGE, stained with Coomassie brilliant blue before destaining, and visualized on a gel reader. The intensity was measured by Image Studio v.5.2.

Western blotting

After running the previous SDS-PAGE gel for an ideal time, proteins were transferred for 30 min at 25 V. The nitrocellulose membrane was blocked with 5% BSA in Tris-buffered saline containing 0.05% Tween 20 and blotted overnight with a primary antibody prepared in tris buffered saline with tween (TBST) containing 2.5% BSA. The membrane was developed using a secondary fluorescent antibody and acquired on an Odyssey CLx imaging system.

Immunoprecipitation

Raji B cells overexpressing PD-L1 and Jurkat T cells overexpressing PD-1 were lysed in cold immunoprecipitation (IP) lysis buffer

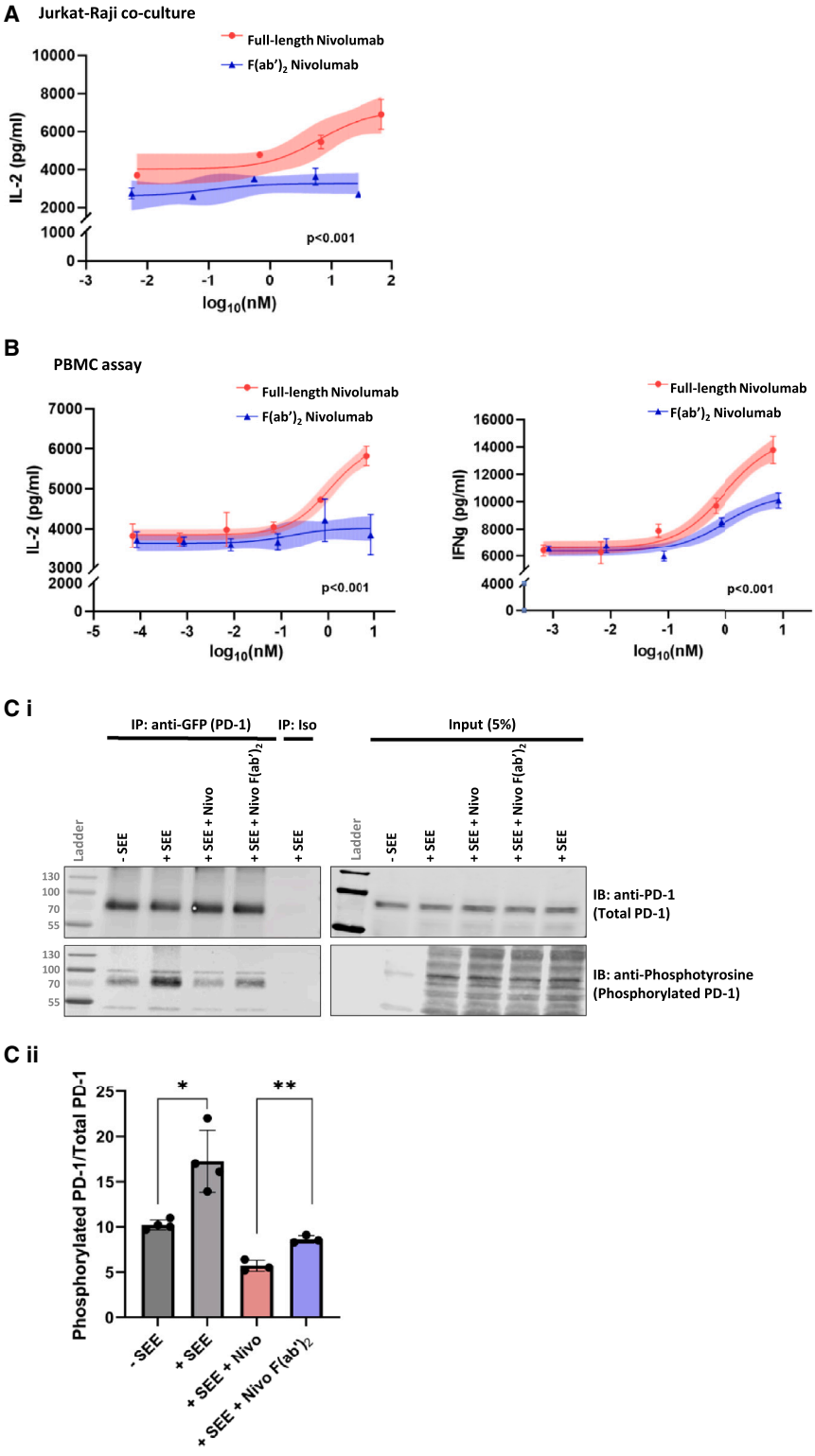

Figure 4. Removing PD-1 from the IS is associated with increased T cell activation

(A) IL-2 levels of Jurkat T cell and Raji B cell with different concentrations of either full-length nivolumab or its F(ab′)$_2$ in the presence of SEE. $n = 3$, $p < 0.001$ (unpaired t test with Welch's correction between the non-linear fitting curves). (B) IL-2 and IFN-gamma levels of human PBMC assay of cells treated with SEE and full-length nivolumab or its F(ab′)$_2$ as indicated and measured by ELISA. $n = 3$, $p < 0.001$ (unpaired t test with Welch's correction between the non-linear fitting curves). (C) A Co-immunoprecipitation (Co-I) experiment of Jurkat T cells treated with SEE or anti-PD-1 antibodies for 5 min, followed by PD-1 precipitation with anti-GFP antibodies and western blotting with anti-4G10 antibodies (Ci). The quantitative analysis of the experiment described in C is shown (Cii). $n = 3$–4 independent experiments, paired two-tailed t test; $^*p < 0.05$, $^{**}p < 0.01$.

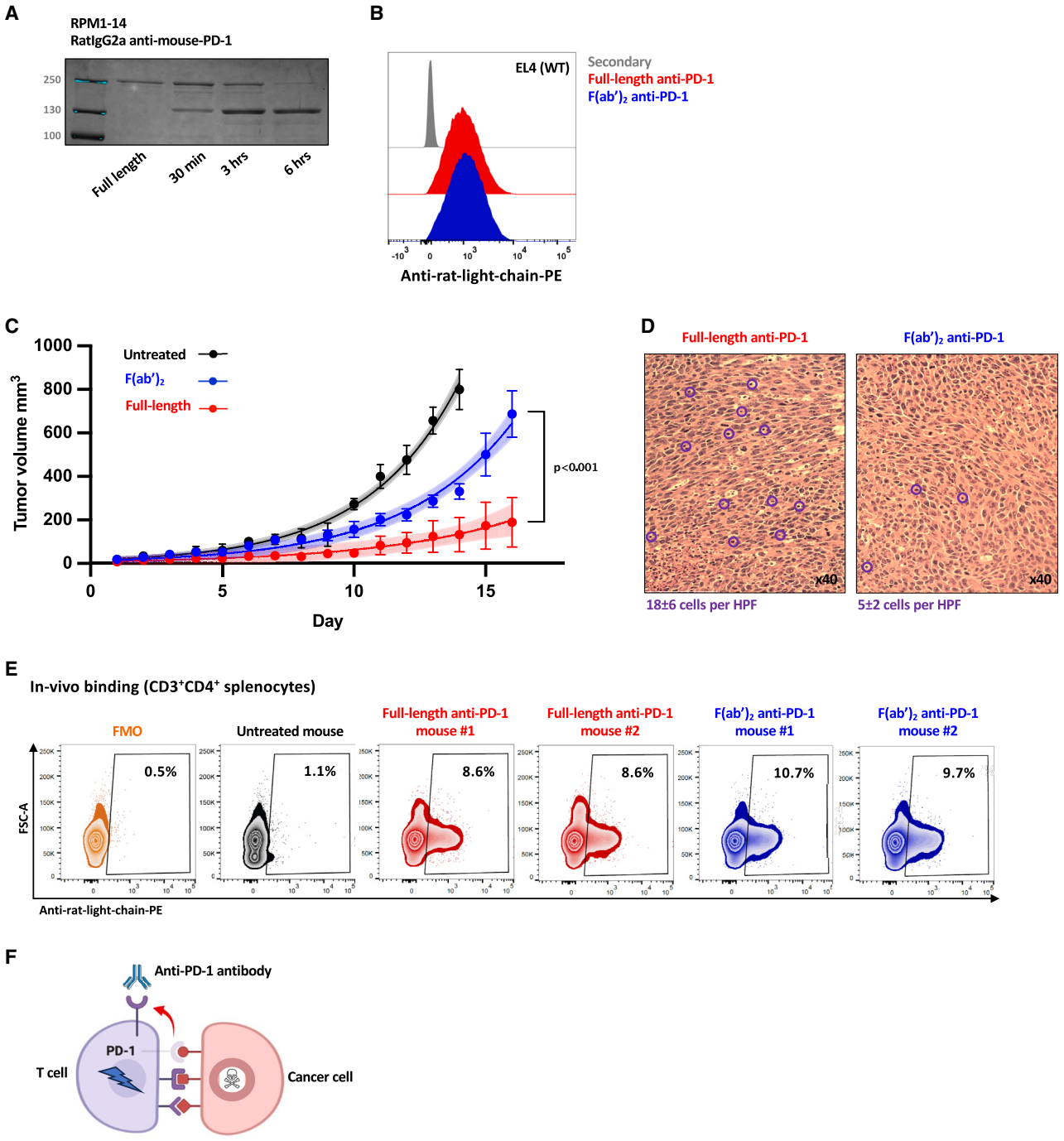

Figure 5. Anti-PD-1 F(ab′)$_2$ cannot inhibit tumor growth *in vivo*

(A) Coomassie staining of non-reduced full-length anti-murine PD-1 treated with pepsin. (B) Flow cytometry of the EL4 murine T cell line treated with the antibodies, as indicated. (C) MC38 syngeneic tumor model showing tumor growth of mice treated with full-length anti-PD-1 antibodies twice a week for four doses or with the same molar amount of anti-murine PD-1 F(ab′)$_2$. $n = 5$, two-way ANOVA. (D) H&E staining of the tumors at the end of the experiment. (E) Flow cytometry of both the full length and the F(ab′)$_2$ versions of the anti-PD-1 antibodies using T cells isolated from the spleens of these mice. The numbers displayed in the boxes are the percentages of the cells bound with the target full length and the F(ab′)$_2$ versions of the anti-PD-1 antibodies. (F) Model for antibody-mediated PD-1 removal from the IS.

(25 mM Tris-HCl, 150 mM NaCl, 1 mM EDTA, 0.5% NP-40, 5% glycerol). The lysis process was carried out at 4°C for 30 min. The lysates were centrifuged for 10 min at 12,000 × *g* and 4°C. Lysates were then used to immunoprecipitate PD-1-GFP using anti-GFP antibody-conjugated agarose beads (MBL) according to the manufacturer's protocol. The PD-1-GFP protein was then separated from the beads by sample buffer (2× Laemmli buffer, boiled at 95°C for 10 min) and loaded onto SDS-PAGE gel with 5% of the input. Five percent of the flowthrough was also loaded (Figure S2).

IL-2 and IFN-gamma ELISA

To determine the concentration of secreted cytokines following different stimulation conditions, a human IL-2 ELISA kit (catalog number 431801, BioLegend) and human interferon (IFN)-gamma kit (catalog number 430101, BioLegend) were used according to the manufacturer protocols.

Flow cytometry

The binding of full-length and fragmented nivolumab was tested using Jurkat-PD-1-GFP cells, the binding of full-length and fragmented durvalumab was tested using Raji-PD-L1-mCherry cells, and the binding of full-length and fragmented anti-mouse-PD-1 was tested using wild-type EL4 cells. In all cases, 0.5 million cells/test were incubated with equal molar concentrations of full-length/fragmented antibodies in fluorescence-activated cell sorting buffer (2% FBS in PBS) for 30 min at 4°C. Following two washes, the cells were stained for 30 min at 4°C with a fluorescently labeled secondary antibody (anti-human immunoglobulin G [IgG]-F(ab′)$_2$ [Jackson ImmunoResearch, 109-606-097, used at 1:400] for nivolumab and durvalumab-stained samples and anti-rat Ig light chain [BioLegend, 407805, used at 1:250] for anti-mouse-PD-1-stained samples), washed twice, and acquired using a BD LSRII flow cytometer. Data were analyzed using FlowJo software (v.10.7.1).

Mice and tumor cell lines

Columbia University Institutional Animal Care and Use Committee approved the animal studies. Female 8-week-old C57BL/6 mice were used. The murine colon adenocarcinoma (MC38) colon carcinoma cells were purchased from Kerafast (catalog number ENH204-FP). The MC38 cells were maintained in DMEM supplemented with heat-inactivated FBS (10%) and penicillin/streptomycin (1% 10,000 U/mL stock) and grown at 37°C with 5% CO_2. Cells were passaged before storage and thawed and passaged twice before implantation for all described tumor experiments. All cell lines were determined to be free of mycoplasma (Lonza).

Tumor model

MC38 (2×10^5) cells were implanted subcutaneously in the right hindflank of 8-week-old B6 (Jax) mice. Tumor growth was monitored using electronic calipers and calculated using V = length × width2 × 0.52. When tumor volume reached 50 mm^3, the mice started receiving treatments (2 doses per week, four doses total) at a molar dose equal 200 μg per dose. Tumor sizes were tracked daily along the course. Mice were eventually sacrificed, and tumors were collected for histology. Each group of mice included 5–7 mice, and the experiment was terminated when the tumor reached a volume of 1,000 mm^3 or after 17 days.

Tumor infiltration histology

For H&E, tumors were fixed in 10% neutral buffered formalin, and then paraffin was embedded and cut into 5-μm sections. Slices were stained with H&E. T cells were qualified by counting mononuclear cells in a high-power field.

Statistics

Values are reported as mean ± SEM. Statistical graphs were analyzed on GraphPad Prism 9 using a paired/unpaired t test (with Welch's correction where applicable) and ANOVA two-way test.

Ethics

The Institutional Review Board at Columbia University Medical Center approved the study, and all donors provided informed consent.

DATA AND CODE AVAILABILITY

All data are available upon reasonable request from the corresponding author.

SUPPLEMENTAL INFORMATION

Supplemental information can be found online at https://doi.org/10.1016/j.omton.2024.200839.

ACKNOWLEDGMENTS

This work was supported by grants from the NIH (AI125640, CA231277, AI150597, AI175498).

AUTHOR CONTRIBUTIONS

L.Y.H. performed the experiments, analyzed the data, and drafted the manuscript. S.L. designed and performed experiments and analyzed the data. M.P., S.B., R.S., E.K.M., M.G., Y.G., and X.H. performed some experiments and improved the overall experiment process. A.M. sketched out the experiments, revised the manuscript, provided material support, and offered reagents and data analysis tools. The manuscript was read, verified, and approved by all authors.

DECLARATION OF INTERESTS

The authors declare no competing interests.

REFERENCES

1. Dustin, M.L., and Baldari, C.T. (2017). The Immune Synapse: Past, Present, and Future. Methods Mol. Biol. *1584*, 1–5.

2. Dustin, M.L. (2010). Insights into function of the immunological synapse from studies with supported planar bilayers. Curr. Top. Microbiol. Immunol. *340*, 1–24.

3. Davis, D.M., Igakura, T., McCann, F.E., Carlin, L.M., Andersson, K., Vanherberghen, B., Sjöström, A., Bangham, C.R.M., and Höglund, P. (2003). The protean immune cell synapse: a supramolecular structure with many functions. Semin. Immunol. *15*, 317–324.

4. Cemerski, S., and Shaw, A. (2006). Immune synapses in T-cell activation. Curr. Opin. Immunol. *18*, 298–304.

5. Kupfer, A., and Kupfer, H. (2003). Imaging immune cell interactions and functions: SMACs and the Immunological Synapse. Semin. Immunol. *15*, 295–300.
6. Valitutti, S. (2008). Immunological synapse: center of attention again. Immunity *29*, 384–386.
7. Cartwright, A.N.R., Griggs, J., and Davis, D.M. (2014). The immune synapse clears and excludes molecules above a size threshold. Nat. Commun. *5*, 5479.
8. Oszmiana, A., Williamson, D.J., Cordoba, S.P., Morgan, D.J., Kennedy, P.R., Stacey, K., and Davis, D.M. (2016). The Size of Activating and Inhibitory Killer Ig-like Receptor Nanoclusters Is Controlled by the Transmembrane Sequence and Affects Signaling. Cell Rep. *15*, 1957–1972.
9. Ritu, Chandra, P., and Das, A. (2023). Immune checkpoint targeting antibodies hold promise for combinatorial cancer therapeutics. Clin. Exp. Med. *23*, 4297–4322.
10. Cai, L., Li, Y., Tan, J., Xu, L., and Li, Y. (2023). Targeting LAG-3, TIM-3, and TIGIT for cancer immunotherapy. J. Hematol. Oncol. *16*, 101.
11. Wang, Y., Du, J., Gao, Z., Sun, H., Mei, M., Wang, Y., Ren, Y., and Zhou, X. (2023). Evolving landscape of PD-L2: bring new light to checkpoint immunotherapy. Br. J. Cancer *128*, 1196–1207.
12. Mestrallet, G., Brown, M., Bozkus, C.C., and Bhardwaj, N. (2023). Immune escape and resistance to immunotherapy in mismatch repair deficient tumors. Front. Immunol. *14*, 1210164.
13. Strazza, M., Azoulay-Alfaguter, I., Peled, M., Adam, K., and Mor, A. (2021). Transmembrane adaptor protein PAG is a mediator of PD-1 inhibitory signaling in human T cells. Commun. Biol. *4*, 672.
14. Davis, D.M., and Dustin, M.L. (2004). What is the importance of the immunological synapse? Trends Immunol. *25*, 323–327.
15. Strazza, M., Moore, E.K., Adam, K., Azoulay-Alfaguter, I., and Mor, A. (2022). Neutralization of the adaptor protein PAG by monoclonal antibody limits murine tumor growth. Mol. Ther. Methods Clin. Dev. *27*, 380–390.
16. Dragovich, M.A., Adam, K., Strazza, M., Tocheva, A.S., Peled, M., and Mor, A. (2019). SLAMF6 clustering is required to augment T cell activation. PLoS One *14*, e0218109.
17. Gartshteyn, Y., Askanase, A.D., Song, R., Bukhari, S., Dragovich, M., Adam, K., and Mor, A. (2023). SLAMF6 compartmentalization enhances T cell functions. Life Sci. Alliance *6*, e202201533.
18. Moore, E.K., Strazza, M., and Mor, A. (2022). Combination Approaches to Target PD-1 Signaling in Cancer. Front. Immunol. *13*, 927265.
19. Riley, J.L. (2009). PD-1 signaling in primary T cells. Immunol. Rev. *229*, 114–125.
20. Peled, M., Tocheva, A.S., Sandigursky, S., Nayak, S., Philips, E.A., Nichols, K.E., Strazza, M., Azoulay-Alfaguter, I., Askenazi, M., Neel, B.G., et al. (2018). Affinity purification mass spectrometry analysis of PD-1 uncovers SAP as a new checkpoint inhibitor. Proc. Natl. Acad. Sci. USA *115*, E468–E477.
21. Patsoukis, N., Wang, Q., Strauss, L., and Boussiotis, V.A. (2020). Revisiting the PD-1 pathway. Sci. Adv. *6*, eabd2712.
22. Azoulay-Alfaguter, I., Strazza, M., Pedoeem, A., and Mor, A. (2015). The coreceptor programmed death 1 inhibits T-cell adhesion by regulating Rap1. J. Allergy Clin. Immunol. *135*, 564–567.
23. Wang, Q., Bardhan, K., Boussiotis, V.A., and Patsoukis, N. (2021). The PD-1 Interactome. Adv. Biol. *5*, e2100758.
24. Badiee, P., Maritz, M.F., and Thierry, B. (2022). Glycogen kinase 3 inhibitor nanoformulation as an alternative strategy to inhibit PD-1 immune checkpoint. Int. J. Pharm. *622*, 121845.
25. Fernandes, R.A., Su, L., Nishiga, Y., Ren, J., Bhuiyan, A.M., Cheng, N., Kuo, C.J., Picton, L.K., Ohtsuki, S., Majzner, R.G., et al. (2020). Immune receptor inhibition through enforced phosphatase recruitment. Nature *586*, 779–784.
26. Barot, S., Patel, H., Yadav, A., and Ban, I. (2023). Recent advancement in targeted therapy and role of emerging technologies to treat cancer. Med. Oncol. *40*, 324.
27. Kamioka, Y., Ueda, Y., Kondo, N., Tokuhiro, K., Ikeda, Y., Bergmeier, W., and Kinashi, T. (2023). Distinct bidirectional regulation of LFA1 and α4β7 by Rap1 and integrin adaptors in T cells under shear flow. Cell Rep. *42*, 112580.
28. Faust, M.A., Rasé, V.J., Lamb, T.J., and Evavold, B.D. (2023). What's the Catch? The Significance of Catch Bonds in T Cell Activation. J. Immunol. *211*, 333–342.
29. Jung, Y. (2023). Pre-organized landscape of T cell surface. Front. Immunol. *14*, 1264721.
30. Jiang, X., Sun, L., Hu, C., Zheng, F., Lyu, Z., and Shao, J. (2023). Shark IgNAR: The Next Broad Application Antibody in Clinical Diagnoses and Tumor Therapies? Mar. Drugs *21*, 496.
31. Tocheva, A.S., Lerrer, S., and Mor, A. (2020). In Vitro Assays to Study PD-1 Biology in Human T Cells. Curr. Protoc. Im. *130*, e103.